NASA TECHNICAL MEMORANDUM

NASA TM X-3515

NASA TM X-3515

ANALYTICAL PREDICTION OF THE PERFORMANCE AND STABILITY OF A J85-13 COMPRESSOR WITH DISTORTED INLET FLOW

Edward J. Milner

Lewis Research Center
Cleveland, Ohio 44135

NATIONAL AERONAUTICS AND SPACE ADMINISTRATION • WASHINGTON, D. C. • MAY 1977

1. Report No. NASA TM X-3515	2. Government Accession No.	3. Recipient's Catalog No.
4. Title and Subtitle ANALYTICAL PREDICTION OF THE PERFORMANCE AND STABILITY OF A J85-13 COMPRESSOR WITH DISTORTED INLET FLOW		5. Report Date May 1977 6. Performing Organization Code
7. Author(s) Edward J. Milner		8. Performing Organization Report No. E-8887 10. Work Unit No. 505-05
9. Performing Organization Name and Address Lewis Research Center National Aeronautics and Space Administration Cleveland, Ohio 44135		11. Contract or Grant No. 13. Type of Report and Period Covered Technical Memorandum
12. Sponsoring Agency Name and Address National Aeronautics and Space Administration Washington, D.C. 20546		14. Sponsoring Agency Code
15. Supplementary Notes		

16. Abstract

This report is part of a trilogy reporting further investigations of the parallel compressor concept. The compressor model used in the study is based on the overall clean-inlet performance map obtained from experimental tests in an altitude chamber using a General Electric J85-13 turbojet engine. The model, which includes a static-pressure balance calculation at compressor discharge, was exercised at conditions corresponding to 10 different screen-induced distortion patterns included in the experimental data base. The spoiled area of these patterns ranged from 30^{o} to 180^{o}, and the distortion screen density, or the area blocked by the screen wire per unit area of screen, varied from 26 to 69 percent. Results of the study indicate that at the higher corrected speeds the analytical surge lines obtained are good representations of the corresponding experimental surge lines - independent of distortion angle or distortion level.

17. Key Words (Suggested by Author(s))	18. Distribution Statement
Parallel compressor - surge line prediction Compressor surge prediction - distorted inlet Surge line prediction - distorted compressor Distortion - compressor surge	Unclassified - unlimited STAR category 07

19. Security Classif. (of this report)	20. Security Classif. (of this page)	21. No. of Pages	22. Price*
Unclassified	Unclassified	29	A03

* For sale by the National Technical Information Service, Springfield, Virginia 22161

ANALYTICAL PREDICTION OF THE PERFORMANCE AND STABILITY OF A J85-13 COMPRESSOR WITH DISTORTED INLET FLOW

by Edward J. Milner

Lewis Research Center

SUMMARY

Simulation techniques implemented on the digital computer were used at Lewis Research Center to further investigate the parallel compressor concept. This report, together with two companion reports, documents results obtained from those studies. The compressor simulation included here was modeled after clean-inlet compressor data included in a data base obtained from experimental tests of a General Electric J85-13 turbojet engine in an altitude chamber at the Lewis Research Center. Also included in the experimental data base were results from 10 different compressor inlet distortion patterns. The spoiled area of the screen-induced circumferential distortion patterns ranged from 30° to 180° sectors. The distortion screen density, or the area blocked by the screen wire per unit area of screen, varied from 26 to 69 percent.

Two features included in the simulation were that (1) each compressor segment was modeled as a single lump based on the experimental overall compressor map and (2) a static pressure balance calculation was included to satisfy the parallel compressor requirement that the static discharge pressure of the individual compressor segments be equal.

The parallel compressor model was exercised using compressor-inlet conditions corresponding to the 10 experimental circumferential distortion patterns. Comparing the analytical results with the corresponding experimental data indicated that at the higher corrected speeds the analytical surge lines are good representations of the corresponding experimental surge lines - independent of distortion angle of extent or distortion level. Hence, the simulation may be used at these higher speeds to evaluate shifts in the surge line due to inlet pressure distortion.

Although the positions of the analytical speed lines with respect to the corresponding experimental data are generally good, a more complex model than that discussed here is apparently required for them to overlay each other. It may be necessary, for example, to develop techniques compatible with the parallel compressor concept which consider crossflow of air between the high-pressure and low-pressure sectors of the compressor.

INTRODUCTION

The trend in modern aircraft has been toward designs that develop higher thrust without sacrificing maneuverability or increasing overall weight. As aircraft have become lighter and more efficient, so have the engines that power them. Engines built using multistage compressors with compact, lightweight cases can deliver exceptional performance. For this reason designers are concentrating a great deal of their effort on the development of compressors that efficiently extract more and more work per stage. However, as engines are becoming smaller and more powerful, a persistent problem in compressor and inlet design is becoming more significant, namely, the adverse effect of inlet pressure distortion on engine performance (ref. 1). Inlet pressure distortion is one of the chief causes of compressor surge in supersonic aircraft. A knowledge of the effect of compressor-face pressure distortion on surge margin and performance is critical to obtaining an optimum design.

The surge margin of a compressor exposed to inlet pressure distortion is affected by both the distortion level and its angle of extent (ref. 2). Surge margin can be obtained experimentally for a given compressor exposed to particular distortion levels and angles of extent; however, such tests are expensive and time consuming. Having to repeat them for each new compressor design is clearly undesirable. Hence, a computer simulation that could be used to investigate the effect on surge margin of any distortion level covering any angle of extent would be most useful.

The parallel compressor concept suggested by Pearson and McKenzie (ref. 3) has been applied to experimental data with promising results. For a given corrected speed the surge pressure ratio of an undistorted compressor was found to correlate very well with the peak pressure ratio encountered at surge by the same compressor exposed to inlet-pressure distortion (ref. 4). The parallel compressor concept is based on the premise that a compressor subjected to inlet pressure distortions can be considered as two (or more) compressors operating in parallel, each having a constant but different inlet total pressure. The theory assumes that (1) no crossflow occurs between the stages of the parallel compressors, (2) each of the parallel compressors operates as an undistorted compressor, and (3) each of the parallel compressors discharges to a common plenum, causing each to have the same static discharge pressure. Surge of the overall compressor is determined when any of the individual parallel compressors surges. Hence, having available the undistorted compressor performance map is essential to applying parallel compressor theory.

In view of encouraging experimental results such as those mentioned previously, simulation techniques implemented on the digital computer were used at Lewis to further investigate the parallel compressor concept. This report and its two companion reports (refs. 5 and 6) document the results obtained from these studies.

A comprehensive data base obtained from experimental tests conducted in an altitude chamber at Lewis using a General Electric J85-13 turbojet engine is presented in reference 5. Each of the eight compressor stages was instrumented to obtain the characteristics of the individual stages. Performance data are presented not only for undistorted inlet flow but also for a variety of inlet distortion patterns covering a wide range of distortion levels.

Daniele (ref. 6) investigated a completely analytical approach to try to determine compressor surge. The technique used required no knowledge of the experimental clean-inlet surge line; however, it did require a stage-by-stage model of the compressor. The Routh-Hurwitz method was used to analytically determine the stability of the system. The simulation model included a stage-by-stage representation of the eight-stage compressor based on the experimental compressor stage characteristics documented in reference 5. A Routh-Hurwitz analysis was used to determine whether the system of equations representing a given operating condition was stable at that point; complete details of the study are included in reference 6.

The results of a parallel compressor study based on the overall performance of the compressor is presented in this report. For this study the compressor is modeled as a single lump based on the experimental overall performance of the clean-inlet compressor. Past investigations at Lewis applying the parallel compressor concept to experimental data have assumed uniform total-pressure conditions at compressor discharge. This assumption was an approximation of the parallel compressor theory requirement that all compressor segments discharge to a common plenum, causing each to have the same static discharge pressure. The simulation model for this study includes a static-pressure balance at compressor discharge. The model was exercised using a variety of inlet distortion patterns, and the resulting surge lines were compared with corresponding surge data from an experimental data base.

EXPERIMENTAL DATA BASE

The experimental data base used for the study discussed in this report was obtained from a series of tests conducted in an altitude chamber at Lewis Research Center and reported in references 5 and 7. Brief descriptions of the experimental engine and the pertinent data are provided in this section for convenience. For a more complete discussion of these topics, however, references 5 and 7 should be consulted.

Engine Geometry

The experimental data base was obtained using a General Electric J85-13 turbojet engine. This engine includes an eight-stage, axial-flow compressor which is equipped

with three controlled interstage bleeds that open and close in unison; the compressor is directly coupled to a two-stage turbine. The engine also has an afterburner section and an exhaust nozzle with a variable throat area. The combustor is a through-flow annular type.

Located in the engine inlet are variable guide vanes, which are mechanically linked to the interstage bleeds in such a way that the bleeds will be fully opened when the guide vanes are rotated to their maximum angle of attack. The interstage bleeds were scheduled to be fully opened below 80 percent corrected speed, to be half-open at 87 percent corrected speed, and to be fully closed above 94 percent corrected speed. This schedule conformed to the manufacturer's suggested schedule, except that its temperature sensitivity had been removed to allow comparison of results without concern over inlet temperature. In addition, the turbine diaphragm area had been reduced by 15 percent to 232 square centimeters to allow the compressor to surge without exceeding temperature limits.

Clean-Inlet Data

The compressor had been mapped and surged with no inlet distortion screens in place except for the large meshed support screen at corrected speeds of 80, 87, 94, and 100 percent. These data, along with a projected surge line based on an extrapolation procedure (ref. 5), were included in the data base. In addition, corresponding values of bleed flow, stage pressures, and stage temperatures were available at selected points along each corrected speed line.

Distorted-Inlet Data

Inlet-pressure distortion was introduced by means of screens mounted in the inlet approximately one duct diameter upstream of the compressor face. This caused a pressure defect in the sector of the compressor covered by the screen. Screens of different porosities and sizes caused pressure defects of different magnitudes and extents. Except for the presence of the screen in the inlet duct upstream of the compressor face, the data taking procedure for these distortion tests was identical to that for the clean-inlet tests. An attempt was made to map and surge the experimental engine at corrected speeds of 80, 87, 94, and 100 percent for each distortion pattern. Likewise, for each distortion pattern the extrapolation procedure was used to predict the surge point at each corrected speed.

SIMULATION DESCRIPTION

The parallel compressor simulation and its requirements will be discussed in this section. The simulation model provides a natural structure for the discussion since it consists of two similar, but separate, compressors operating in parallel according to certain constraints. First, the discussion will focus on an individual compressor segment. Then, considerations that must be satisfied by two such compressor segments operating in parallel will be discussed.

Compressor Segment Model

Each compressor segment forming the parallel compressor model is represented as a single lump, the overall performance of each being included in the simulation. Experimental data required to model each compressor segment are a compressor performance map, a bleed-flow schedule, and a discharge temperature schedule. The last two schedules are used in calculating static pressure at compressor discharge.

Compressor performance map. - The simulation of each compressor segment is based on the clean-inlet compressor map from the experimental data base (refs. 5 and 7). The experimental compressor map consists of four corrected speed lines (80, 87, 94, and 100 percent of rated) and the corresponding surge line. These data are presented in figure 1. Notice that the performance map is in terms of discharge total pressure. A calculation to obtain the corresponding static pressure is required because parallel compressor theory assumes a compressor performance map in terms of discharge static pressure.

Bleed flow. - Bleed-flow ratio is scheduled as a function of bleed-valve opening, which in turn is a function of corrected speed. Both of these maps are shown in figures 2 and 3, respectively. The term "bleed-flow ratio" denotes the total weight flow of air through the interstage bleed valves normalized to the total weight flow of air through the compressor inlet. Airflow at compressor discharge is obtained as compressor-inlet airflow less the airflow exhausted through the interstage bleeds.

Discharge temperature. - Temperature ratio is scheduled as a function of both corrected airflow and corrected speed. The temperature ratio is the compressor-discharge total temperature normalized to the compressor-inlet total temperature. The data map includes four corrected speed lines (80, 87, 94, and 100 percent of rated) and is presented in figure 4.

Parallel Compressor Model

The parallel compressor model is formed using two compressor segments operating simultaneously, and discharging to a common plenum. One compressor segment, C', is used to represent performance in the high-pressure region, and the second compressor segment, C'', is used to represent performance in the low-pressure region. (All symbols used in this report are defined in the appendix.) Inlet total pressure and temperature conditions for each compressor segment are determined by the circumferential distortion pattern being studied. No inlet-temperature distortion is considered in the model; $T_2'' = T_2' = \overline{T}_2$ is assumed. Thus, given P_2', P_2'', $\overline{T}_2$, and a level of static discharge pressure $P_{3,s}^*$, the proper airflow split, $\dot{w}_2'$ and $\dot{w}_2''$, must be determined in the simulation so that the static pressures at compressor discharge satisfy the relation $P_{3,s}' = P_{3,s}'' = P_{3,s}^*$.

Because the experimental clean-inlet compressor map (fig. 1) is in terms of total conditions only, static pressure at compressor discharge was determined from Mach number M which in turn was obtained using the well-known relationship:

$$\frac{\dot{w}\sqrt{\gamma g R T}}{C_d \gamma g_c P A} = \frac{M}{\left[1 + \left(\frac{\gamma - 1}{2}\right) M^2\right]^{(\gamma+1)/2(\gamma-1)}} = \frac{M}{\left(1 + 0.2M^2\right)^3} \qquad (\text{for } \gamma_{air} = 1.4) \qquad (1)$$

Figure 5 presents a graph of $M/(1 + 0.2M^2)^3$ versus M.

The procedure used in the parallel compressor simulation for obtaining the performance map of a compressor exposed to circumferential inlet distortion is as follows: For a given corrected speed N_c the inlet conditions P_2', P_2'', and $\overline{T}_2$, together with β, are simulation inputs whose values are fixed by the distortion pattern being studied. An arbitrary point X_i'' is selected on speed line N_c from the clean-inlet compressor map (fig. 1). The corresponding corrected airflow $\dot{w}_{2,c}$ after attenuation by β is chosen as the inlet airflow $\dot{w}_{2,c}''$ of C'', the compressor segment representing operation in the low-pressure region ($\dot{w}_{2,c}'' = \beta \dot{w}_{2,c}$).

Note that, if the data base clean-inlet compressor performance map had been in terms of discharge static pressure $P_{3,s}$, once X_i'' is chosen discharge static pressure $P_{3,s}''$ could be obtained directly. Dividing $P_{3,s}' = P_{3,s}''$ by P_2' would then locate the operating point of C', the compressor segment representing operation in the high-pressure region. However, since the clean-inlet performance map is in terms of total pressures, a different method is required. Once the point X_i'' is chosen, discharge total pressure of the low-pressure segment C'' is fixed. Total temperature and total airflow at compressor discharge are determined using appropriate maps (figs. 2 to 4).

These values are then used in conjunction with equation (1) to obtain the Mach number at compressor discharge, from which $P''_{3,s}$ can be calculated. For the analysis reported here a value of $C_d = 1$ was assumed.

The corresponding operating point for the high-pressure segment C' is obtained through iteration. As an initial guess, a point X'_i with more surge margin than X''_i is chosen on speed line N_c. The corresponding corrected airflow after attenuation by $(1 - \beta)$, $\dot{w}'_{2,c}$, is assumed to be the inlet flow to the high-pressure segment. Tentative values of P'_3, T'_3, $\dot{w}'_3$, and $P'_{3,s}$ are obtained using appropriate maps (figs. 1 to 4). If necessary, X'_i is adjusted and the process repeated until the calculated value of $P'_{3,s}$ converges to $P''_{3,s}$.

Once static pressure balance is achieved, the performance characteristics of the two compressor segments are combined in the following manner to obtain the overall performance of the parallel compressor model C*:

$$P^*_3 = \beta P''_3 + (1 - \beta)P'_3 \tag{2}$$

$$\dot{w}^*_3 = \dot{w}''_3 + \dot{w}'_3 \tag{3}$$

$$T^*_3 = \frac{(\dot{w}''_3 T''_3 + \dot{w}'_3 T'_3)}{\dot{w}^*_3} \tag{4}$$

$$P^*_2 = \beta P''_2 + (1 - \beta)P'_2 \tag{5}$$

$$\dot{w}^*_2 = \dot{w}''_2 + \dot{w}'_2 \tag{6}$$

$$T^*_2 = T''_2 = T'_2 \tag{7}$$

Corresponding flows are simply summed to obtain mean values of flow while mean values of pressure and temperature are area-weighted and flow-weighted averages, respectively.

The coordinate pair $(\dot{w}^*_2, P^*_3/P^*_2)$ defines a point corresponding to a corrected speed N_c on the performance map of C*. The entire N_c line can be defined by choosing other values of X''_i over its range and repeating the procedure just described. Surge occurs in C* when X''_i is chosen as the surge point on the experimental clean-inlet compressor map (fig. 1).

Exercising the parallel compressor model with no distortion present ($P''_2 = P'_2$) re-

sults in an analytical compressor performance map that is identical to the experimental clean-inlet compressor map presented in figure 1.

RESULTS AND DISCUSSION

The experimental data base (ref. 5) includes performance maps of the compressor exposed to the 10 inlet-pressure circumferential distortion patterns summarized in table I. Angles of extent of distortion patterns tested ranged from 30° to 180°; distortion levels were modulated by means of screens whose density, or area blocked by the screen wire per unit area of screen, varied from 26 to 69 percent. The pressure drop characteristics across each of the distortion screens are presented in table II. Exercising the parallel compressor simulation using inlet conditions associated with each of the 10 different distortion patterns yielded the analytical performance maps in figure 6. Each map also shows the corresponding experimental data from reference 5.

To evaluate these results more easily, it is desirable to use some means of quantitatively comparing the relative error between the simulation surge line and that suggested by the corresponding experimental points. A formulation based on the normal from an experimental surge point to the analytical surge line could serve as a measure of the relative error between the analytical and experimental surge lines at that point. One such formulation that could be applied to the data in this report is the following:

$$E = 100\sqrt{\left[\frac{\left(\overline{P}_3/\overline{P}_2\right)_{exp} - \left(\overline{P}_3/\overline{P}_2\right)_n}{\left(\overline{P}_3/\overline{P}_2\right)_{max}}\right]^2 + \left(\frac{\dot{w}_{c,exp} - \dot{w}_{c,n}}{\dot{w}_{c,max}}\right)^2} \tag{8}$$

where the pressure ratio and corrected airflow are normalized to the corresponding maximum value realized by each of these parameters, where the subscript exp denotes the coordinates of the experimental surge point, and where the subscript n denotes the point at which its normal intersects the simulation surge line. The largest value of corrected airflow (19.57 kg/sec) is obtained from the condition represented in figure 6(b), and the largest value of pressure ratio (7.52) is obtained from the condition represented in figure 6(c). Table III presents results obtained from evaluating equation (8) at each surge point in the experimental data base.

180° Distortion Patterns

Circumferential patterns with an angle of extent of 180° were studied at three different distortion levels based on screen densities of 49, 42, and 26 percent. Compressor performance maps for these conditions are presented in figures 6(a) to (c).

The 49 percent density screen, which produced the highest level of distortion, shows excellent agreement between the analytical surge line and the experimental surge points (fig. 6(a)). At corrected speeds of 80, 87, and 100 percent, the analytical speed lines are in good agreement with the corresponding experimental data. However, the shape of the curve suggested by the 94 percent experimental data is unusual compared with the experimental data at the other corrected speeds. One would expect the 94 percent data to form a smooth transition from low corrected speed to high corrected speed (ref. 5).

The 42 percent density screen (fig. 6(b)) has the next highest level of distortion. The analytical surge line for this pattern is more conservative (relative to the experimental surge line) at 80 and 87 percent corrected speeds than that obtained for the 49-percent density screen. (From table III, E has the values 1.98 and 1.36 as opposed to 0.97 and 0.95, respectively.) The 80 percent analytical speed line displays about 1 percent less pumping capacity than that indicated by the experimental data, and the 87 percent analytical speed line agrees well with the experimental data. Here again, the 94 percent corrected speed experimental data display the same unusual characteristics that were found for the 49 percent density screen. Moreover, the 100 percent experimental data suggest a speed line with positive slope, contradicting what experience has shown one to expect. However, the analytical, 100-percent-corrected-speed line has negative slope and agrees well with the higher pressure ratio experimental data, the analytical surge line being in excellent agreement with the experimental surge point.

The 26 percent density screen (fig. 6(c)) produced the lowest level of distortion. For this configuration the analytical surge line is in very good agreement with the experimental surge points. (No experimental surge point is shown at 87 percent corrected speed because a temperature limit was reached before surge occurred.) Furthermore, the 80, 87, and 100 percent analytical speed lines aline very well with the corresponding experimental data. The differences between the analytical and experimental data at 94 percent corrected speed noted at the other two higher distortion levels are not present for this case; the experimental data are scattered about the analytical 94 percent speed line.

90° Distortion Patterns

Figure 6(d) presents the compressor map resulting from the distortion pattern

having a screen density of 49 percent. The analytical surge line seems in acceptable agreement with the experimental surge points at 94 and 100 percent corrected speeds (E = 1.48 and 1.14), but is conservative at 80 percent, and is marginal at 87 percent corrected speeds (E = 2.48 and 1.79, respectively). The experimental data points are scattered about the 87 percent analytical speed line and about the 80 percent analytical speed line at the higher pressure ratios. The analytical speed lines and the experimental data differ significantly at 94 and 100 percent corrected speeds, the 100 percent experimental data suggesting a curve with limited variation in pressure ratio for a wide range in corrected flow.

The compressor map corresponding to a distortion screen density of 42 percent is presented in figure 6(e). Here one observes the analytical surge line being very conservative at 80 and 87 percent corrected speeds (E = 2.87 and 3.00) but in good agreement with the experimental surge points at 94 and 100 percent corrected speeds (E = 0.94 and 0.14). The analytical speed line and the experimental data are in excellent agreement at 87 percent corrected speed. At 80 percent corrected speed the analytical speed line suggests a pumping capacity less than that of the experimental data at the lower pressure ratios. As observed previously for the 180^{o} distortion cases, the analytical speed lines at 94 and 100 percent for these cases also differ from the corresponding experimental data - the 100 percent experimental data again suggesting a curve with limited variation in pressure ratio for a wide range in corrected flow.

For a 26 percent density screen (fig. 6(f)), the analytical surge line and the experimental surge points are in good agreement (E = 0.28 and 0.84, respectively). Here again, one observes no experimental surge point at either 80 or 87 percent corrected speed because temperature limits were reached before surge occurred. The analytical speed lines and the corresponding experimental data are in excellent agreement at both 80 and 87 percent corrected speeds. At 94 percent corrected speed this screen shows the best agreement between the analytical speed line and the experimental data for the three different screen densities studied at this distortion angle. However, at 100 percent corrected speed the experimental data suggest slightly less pumping capacity than does the corresponding analytical speed line.

Patterns with Smaller Distortion Angles

Figure 6(g) presents the compressor map resulting from a distortion angle of 60^{o} with a screen density of 49 percent. The analytical surge line is very conservative for this case at the 80 and 87 percent corrected speeds (E = 3.68 and 3.00, respectively). Nevertheless, at these two speeds the analytical speed lines are in very good agreement with the corresponding experimental data. At the 94 and 100 percent corrected speeds

the analytical surge line is in very good agreement with the experimental surge points (E = 1.25 and 0.68). However, the experimental data suggest less pumping capacity than do the corresponding analytical speed lines; in addition, the experimental data at these speeds suggest curves with limited variation in pressure ratio for a wide range in corrected flow.

The compressor map resulting from a 60° distortion with 42 percent screen density is presented in figure 6(h). Here again the analytical surge line is very conservative at the two lower corrected speeds (E = 2.07 and 3.14), while showing good agreement with the experimental surge points at 94 and 100 percent corrected speeds (E = 0.95 and 0.85). For this case the analytical speed line and the experimental data are in very good agreement at 87 percent corrected speed. Moreover, the experimental data at 80, 94, and 100 percent corrected speeds suggest curves similar in shape to the corresponding analytical speed lines. However, at 80 percent corrected speed the experimental data suggest slightly more pumping capacity than the corresponding analytical speed line. The opposite is true at the 94 and 100 percent corrected speeds: the pumping capacity suggested by these experimental data is slightly less than that of the corresponding analytical speed lines.

The experimental data in figure 6(i) represent an attempt at obtaining a compressor performance map for a 60° distortion with a screen density of 69 percent. It was felt that, although that screen density represented a high distortion level, its harshness might be offset by combining it with a relatively small distortion angle in order to experimentally obtain a compressor performance map. As can be seen from the figure, the mapping was successful at 80 and 87 percent corrected speeds. However, only one point was obtained at 94 percent corrected speed before a turbine temperature limit was encountered, and no points at all could be obtained at a corrected speed of 100 percent for the same reason. Once again the analytical surge line is observed to be very conservative at the lower corrected speeds. The analytical and experimental speed lines are in excellent agreement at 87 percent corrected speed; however, at 80 percent corrected speed the experimental data suggest more pumping capacity than does the corresponding analytical speed line.

Figure 6(j) presents the compressor map resulting from a 30° distortion pattern with a screen density of 42 percent. The analytical surge line agrees well with the experimental surge point at 100 percent corrected speed (E = 1.12), is conservative at 94 percent corrected speed (E = 2.31), and is extremely conservative at the two lower corrected speeds (E = 3.85 and 5.58, respectively). At 87, 94, and 100 percent corrected speeds the analytical speed lines and the experimental data are in excellent agreement, however. At 80 percent corrected speed the experimental data suggest slightly higher pumping capacity than does the analytical speed line.

Evaluation of Parallel Compressor Results

The detailed discussion just completed points out the results summarized in table IV. In general, the analytical surge lines obtained from the parallel compressor simulation described in this report agree very well with the corresponding experimental surge points at 94 percent and 100 percent corrected speeds for each inlet pressure distortion considered. However, for distortion angles less than 180° the simulation is inadequate at the two lower corrected speeds of 80 and 87 percent.

Considering only the 80 and 87 percent corrected speed lines for the moment, one observes that, when the distortion angle is 180°, there is generally good agreement between the analytical surge line and the corresponding experimental surge points at each of the distortion levels studied; yet even though acceptable agreement is achieved at these speeds, the analytical surge line tends to be slightly conservative at each distortion level. For distortion angles of extent of 90°, 60°, and 30°, the analytical surge line obtained from the parallel compressor simulation is too conservative compared with the experimental surge points. These results are consistent with the observations of Melick (ref. 8) and Korn (ref. 9).

On the other hand, considering only the 94 and 100 percent corrected speeds, one observes that for the smaller angles of extent the analytical speed lines suggest higher pumping capacity than does the corresponding experimental data. However, the analytical surge line is generally in excellent agreement with the corresponding experimental surge points for these and all of the other circumferential distortion operating points included in the data base. The overall results indicate that the surge lines obtained from the simulation at these higher corrected speeds are good representations of the corresponding experimental surge lines, independent of distortion angle of extent or distortion level.

This result suggests an important application for the parallel compressor simulation described in this report. Since the rotor speeds of particular interest for the General Electric J85-13 turbojet engine are in the neighborhood of 100-percent-corrected rated speed for that engine (16 500 rpm), the parallel compressor simulation could be used at the higher corrected speeds to evaluate shifts in the surge line due to inlet pressure distortion. As an example, figure 7 presents a family of analytical surge lines corresponding to a distortion angle of extent of 180°, the distortion angle displaying good agreement between the simulation surge line and the corresponding experimental surge points in figure 6(a) to (c), not only at the higher corrected speeds, but also at the lower corrected speeds. Surge lines corresponding to the clean inlet and 2.5, 5.0, 7.5, and 10.0 percent distortion levels (defined as $(P_2' - P_2'')/P_2^*$) are presented in the figure. Deviation from the clean-inlet surge line represents the loss in surge margin due to the inlet pressure distortion level being considered. This information can be used to deter-

mine throttle acceleration schedules to keep the compressor from surging.

Before concluding this section, a few closing remarks are in order. As discussed previously, the compressor model described in this report included a static pressure balance calculation to satisfy the uniform static discharge pressure assumption of parallel compressor theory. Surge lines obtained using the model were good representations of the corresponding experimental surge lines at the higher corrected speeds for all distortion patterns considered. This result is significant in that at these speeds one can use the simulation model to obtain surge lines without concern about distortion level or distortion extent. However, even with the static pressure balance included in the model, in most cases the analytical speed lines do not completely overlay the corresponding experimental speed line data. In some instances one observes analytical speed lines with a pumping capacity different from that suggested by the experimental data. In other instances, the range in pressure ratio of the analytical speed lines is different from that of the experimental data. Apparently, a more complex model than that discussed here is required to eliminate these speed line differences. It may be necessary to develop techniques that are compatible with the parallel compressor concept and that, for example, consider crossflow of air between the high-pressure and low-pressure sectors of the compressor.

SUMMARY OF RESULTS

A digital simulation was developed to further investigate the parallel compressor analysis concept. The compressor simulation was modeled using clean-inlet compressor data included in a data base obtained from experimental tests using a General Electric J85-13 turbojet engine in an altitude chamber at Lewis Research Center.

Two features included in the simulation were (1) each compressor segment was modeled as a single lump based on the experimental overall compressor map, and (2) a static pressure balance calculation was included to satisfy the parallel compressor requirement that the static discharge pressure of the individual compressor segments be equal.

The parallel compressor model was exercised using compressor-inlet conditions corresponding to the 10 different circumferential distortion patterns included in the data base. Comparing the analytical results with the corresponding experimental data led to the following observations (summarized in table IV):

1. At the higher corrected speeds the analytical surge lines are good representations of the corresponding experimental surge lines - independent of distortion angle of extent or distortion level.

2. At the higher corrected speeds the positions of the analytical speed lines are generally in good agreement with the corresponding experimental data for the larger distortion angles. However, for the smaller distortion angles the analytical speed lines generally exhibit greater pumping capacity than does the corresponding experimental data.

3. At the lower corrected speeds and larger distortion angles, the analytical surge lines are generally in good agreement with the corresponding experimental data. However, the analytical surge lines are too conservative at the smaller distortion angles.

4. At the lower corrected speeds the positions of the analytical speed lines generally agree well with the corresponding experimental data.

5. This report is an examination of the analytical surge lines obtained from a parallel compressor model compared with corresponding surge data obtained from experimental distortion tests. (Speed line matching is not addressed.) A more complex model than that discussed here is apparently required for the analytical and experimental speed lines to overlay each other. It may be necessary, for example, to develop techniques compatible with the parallel compressor concept that consider crossflow of air between the high-pressure and low-pressure sectors of the compressor.

Lewis Research Center,
National Aeronautics and Space Administration,
Cleveland, Ohio, December 9, 1976,
505-05.

APPENDIX - SYMBOLS

A	cross-sectional area, m^2
BVO	bleed valve opening
C	compressor segment
C_d	flow coefficient
E	measure of relative error between analytical and experimental surge lines
g	gravitational constant, 9.81 m/sec^2
g_c	gravitational conversion factor, $1(kg \cdot m)/(N \cdot sec^2)$
M	Mach number
N	percent of rated engine speed (16 500 rpm)
P	total pressure, N/m^2
P_s	static pressure, N/m^2
R	universal gas constant, 29.2 m/K
T	total temperature, K
$\dot{w}$	mass flow, kg/sec
X_i	point on compressor map
β	ratio of distortion angle of extent to 360^o
γ	ratio of specific heats

Subscripts:

air	air property
bleed	bleed property
c	corrected to inlet conditions
exp	denotes experimental surge point
max	maximum
n	normal
s	static condition
2	compressor-inlet station
3	compressor-discharge station

Superscripts:

' high-pressure sector

'' low-pressure sector

* overall parallel compressor model

$\bar{}$ mean value

REFERENCES

1. Willoh, Ross: Engine Systems Technology. Aeronautical Propulsion. NASA SP-381, 1975, pp. 329-385.

2. Calogeras, James E.; Mehalic, Charles M.; and Burstadt, Paul L.: Experimental Investigation of the Effect of Screen-Induced Total-Pressure Distortion on Turbojet Stall Margin. NASA TM X-2239, 1971.

3. Pearson, H.; and McKenzie, A. B.: Wakes in Axial Compressors. J. R. Aeron. Soc., vol. 63, no. 583, July 1959, pp. 415-416.

4. Calogeras, James E.; Johnson, Roy L.; and Burstadt, Paul L.: Effect of Screen-Induced Total-Pressure Distortion on Axial-Flow Compressor Stability. NASA TM X-3017, 1974.

5. Milner, Edward J.; and Wenzel, Leon M.: Performance of a J85-13 Compressor with Clean and Distorted Inlet Flow. NASA TM X-3304, 1975.

6. Daniele, Carl J.; and Teren, Fred: Prediction of Compressor Stall for Distorted and Undistorted Inlet Flow. J. Aircraft, vol. 12, no. 10, Oct. 1975, pp. 841-846.

7. Wenzel, Leon M.; Moss, John E., Jr.; and Mehalic, Charles M.: Effect of Casing Treatment on the Performance of a Multistage Compressor. NASA TM X-3175, 1975.

8. Melick, H. C., Jr.; and Simpkin, W. E.: A Unified Theory of Inlet/Engine Compatability. AIAA Paper 72-1115, Nov.-Dec. 1972.

9. Korn, James A.: Compressor Distortion Estimates Using Parallel Compressor Theory and Stall Delay. J. Aircraft, vol. 11, no. 9, Sept. 1974, pp. 584-586.

TABLE I. - SUMMARY OF SCREEN PATTERN INFORMATION

FOR CIRCUMFERENTIALLY DISTORTED INLET

Angle of extent, deg	Spoiled-area ratio, percent	Distortion screen density, percent blockage	Figure
180	50	49	6(a)
		42	6(b)
		26	6(c)
90	25	49	6(d)
		42	6(e)
		26	6(f)
60	$16\frac{2}{3}$	49	6(g)
		42	6(h)
		69	6(i)
30	$8\frac{1}{3}$	42	6(j)

TABLE II. - DISTORTION SCREEN CHARACTERISTICS

AT MAXIMUM ANGLE OF EXTENT

Distortion screen density, percent	Mean corrected speed, percent of rated	Mean pressure ratio across screen
26	80.0	0.978
	87.1	.970
	94.2	.961
	100.0	.947
42	80.1	0.959
	87.1	.942
	94.0	.925
	100.1	.894
49	80.0	0.950
	87.0	.930
	94.0	.907
	100.1	.870
69	80.0	0.926
	87.1	.898
	94.1	.868

TABLE III. - SUMMARY OF RELATIVE ERROR BETWEEN ANALYTICAL AND EXPERIMENTAL SURGE LINES AT EACH OPERATING CONDITION

Distortion angle of extent, deg	Distortion screen density, percent	Corrected rotor speed, percent of rated	Measure of relative error between analytical and experimental surge lines (eq. (8)), E	Figure
180	49	80	0.97	6(a)
		87	.95	
		94	.71	
		100	.84	
	42	80	1.98	6(b)
		87	1.36	
		94	2.18	
		100	.97	
	26	80	0.98	6(c)
		94	.14	
		100	1.11	
90	49	80	2.48	6(d)
		87	1.79	
		94	1.48	
		100	1.14	
	42	80	2.87	6(e)
		87	3.00	
		94	.94	
		100	.14	
	26	94	0.28	6(f)
		100	.84	
60	49	80	3.68	6(g)
		87	3.00	
		94	1.25	
		100	.68	
	42	80	2.07	6(h)
		87	3.14	
		94	.95	
		100	.85	
	69	80	3.42	6(i)
		87	3.77	
30	42	80	3.85	6(j)
		87	5.58	
		94	2.31	
		100	1.12	

TABLE IV. - COMPARISON OF ANALYTICAL AND EXPERIMENTAL RESULTS FOR DIFFERENT COMBINATIONS OF DISTORTION ANGLE AND CORRECTED ROTOR SPEED

Distortion angle	High corrected speed	Low corrected speed
Large	Good surge line prediction Generally good speed line agreement	Generally good surge line prediction Generally good speed line agreement
Small	Good surge line prediction Pumping capacity of analytical characteristics generally high	Analytical surge line conservative Generally good speed line agreement

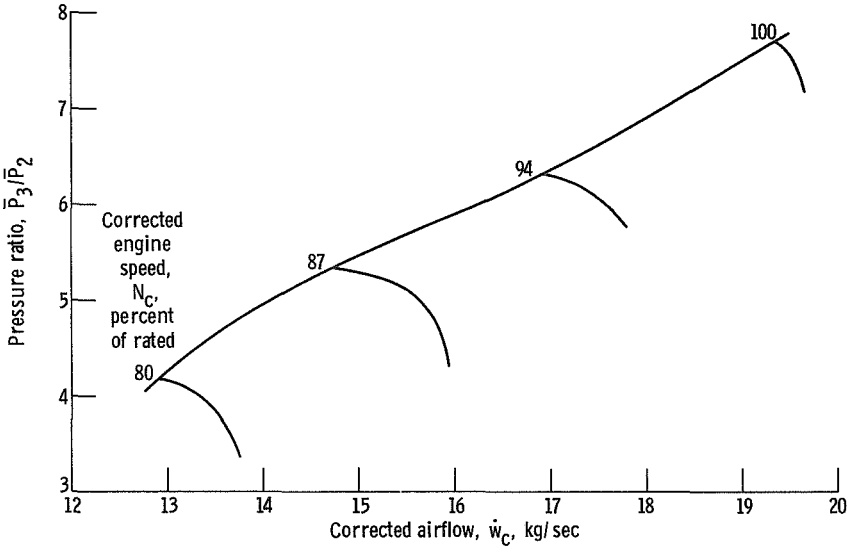

Figure 1. - Experimental compressor map with extrapolated surge line.

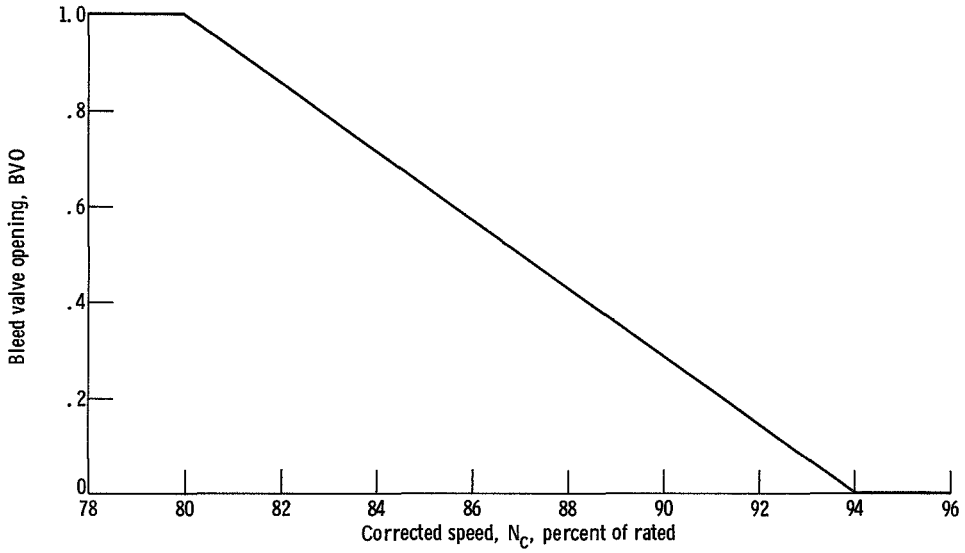

Figure 2. - Compressor bleed valve opening as function of corrected engine speed.

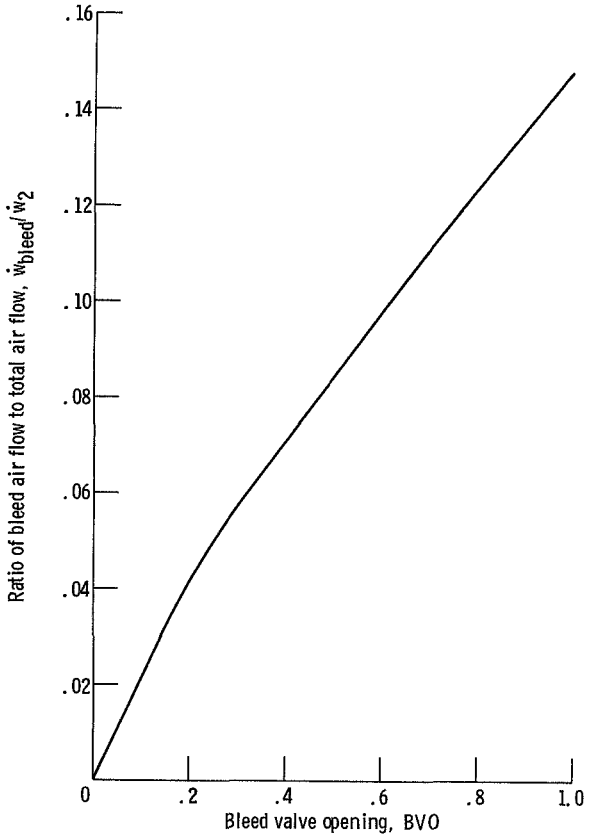

Figure 3. - Bleed flow ratio as function of compressor bleed valve opening.

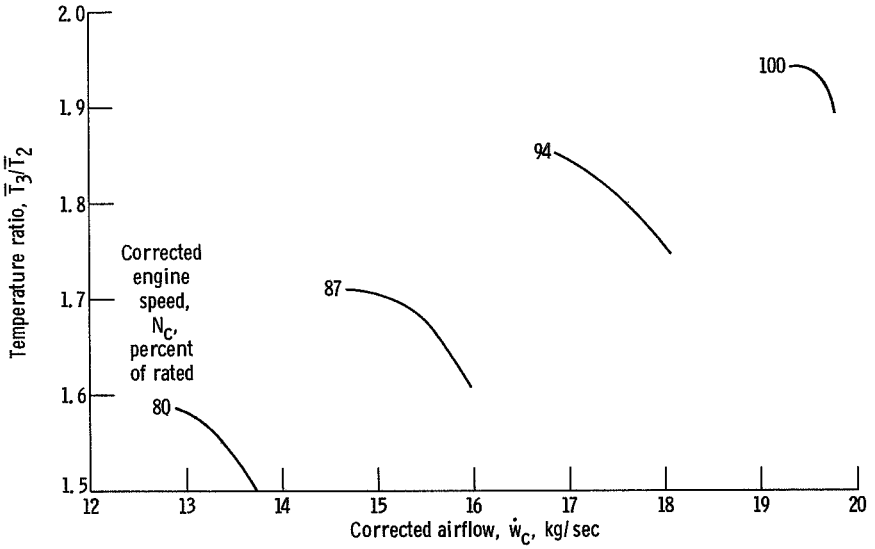

Figure 4. - Compressor temperature ratio as function of corrected airflow and corrected engine speed.

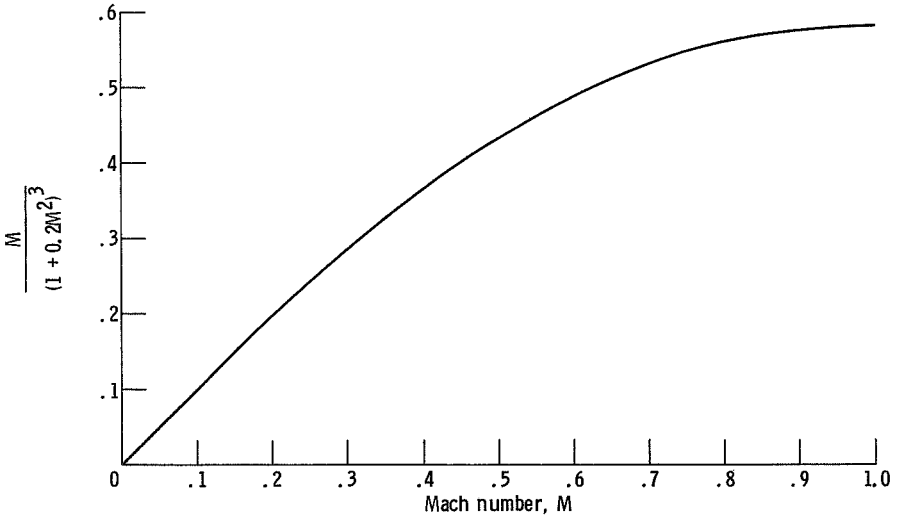

Figure 5. - $\frac{M}{(1+0.2M^2)^{\frac{3}{2}}}$ as function of Mach number.

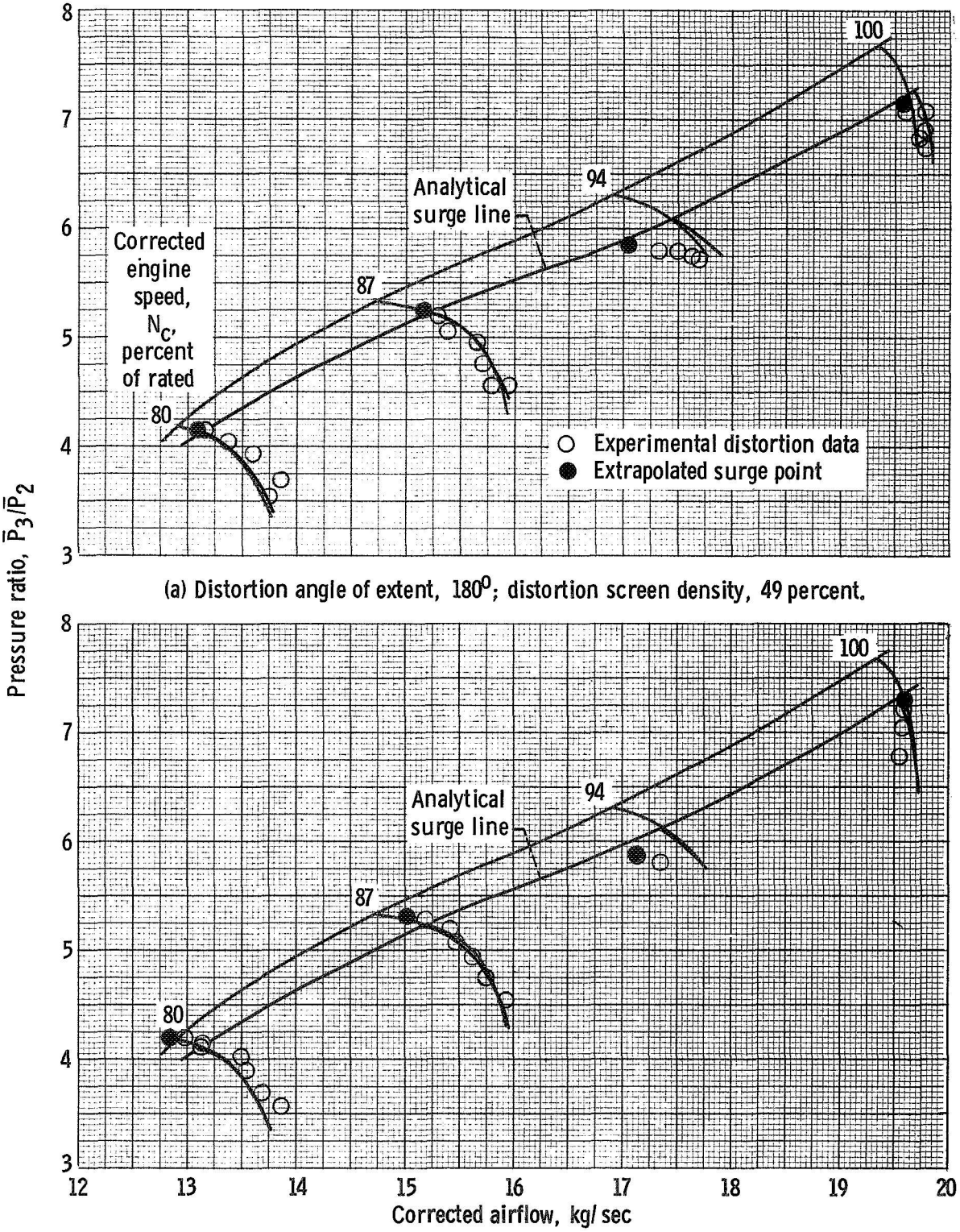

(a) Distortion angle of extent, 180°; distortion screen density, 49 percent.

(b) Distortion angle of extent, 180°; distortion screen density, 42 percent.

Figure 6. - Analytical compressor map superimposed on corresponding experimental points and experimental clean-inlet compressor map.

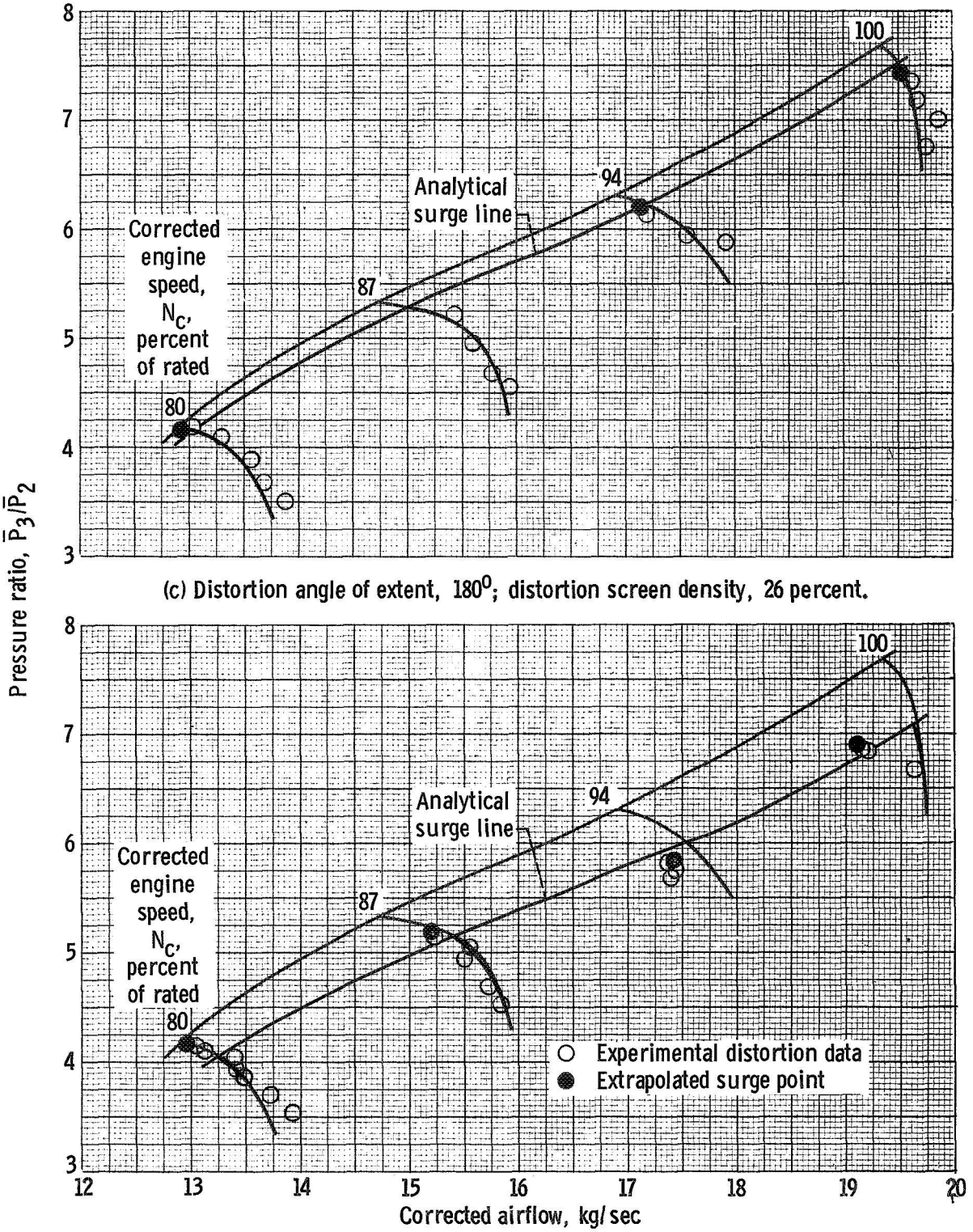

(c) Distortion angle of extent, 180°; distortion screen density, 26 percent.

(d) Distortion angle of extent, 90°; distortion screen density, 49 percent.

Figure 6. - Continued.

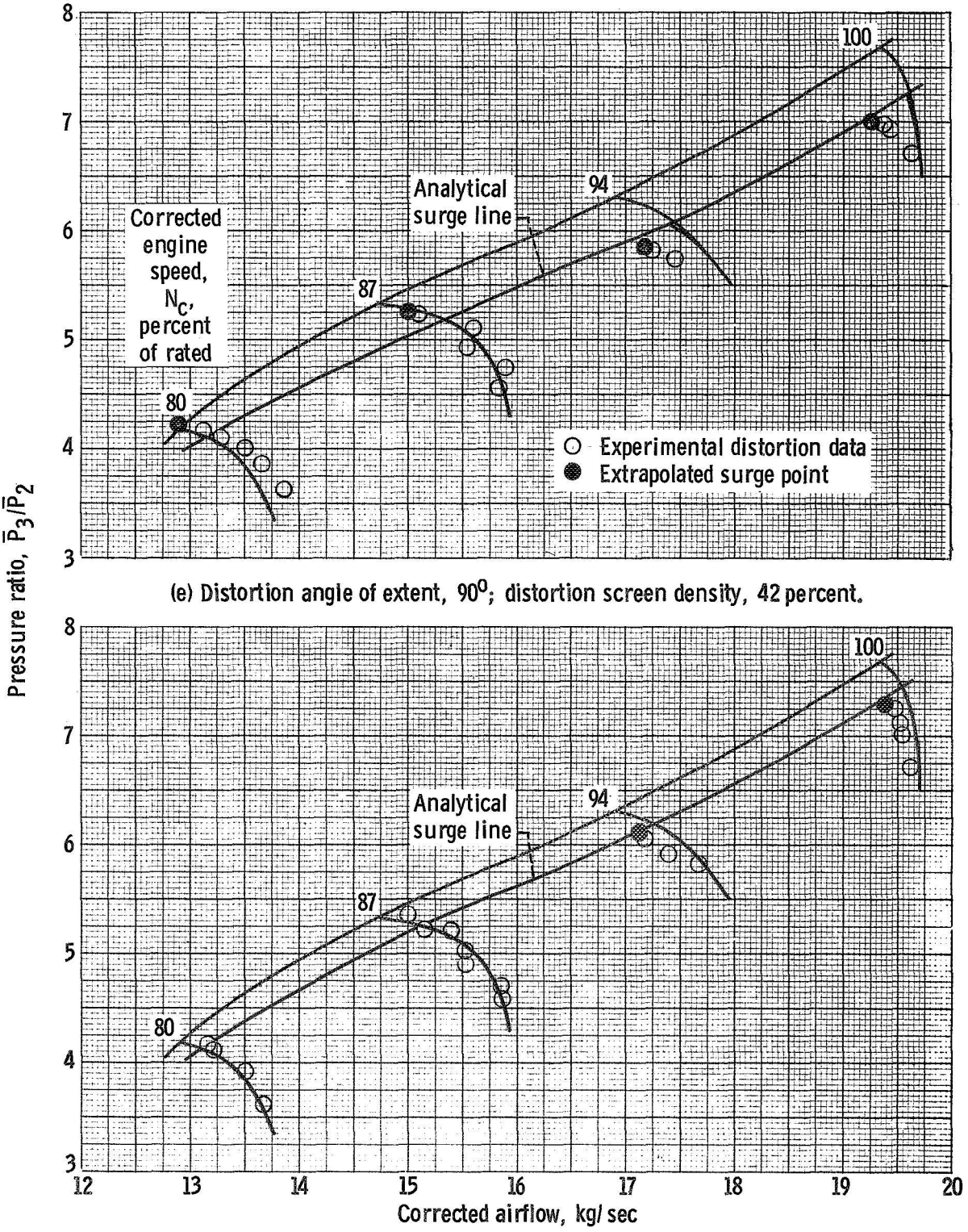

(e) Distortion angle of extent, 90°; distortion screen density, 42 percent.

(f) Distortion angle of extent, 90°; distortion screen density, 26 percent.

Figure 6. - Continued.

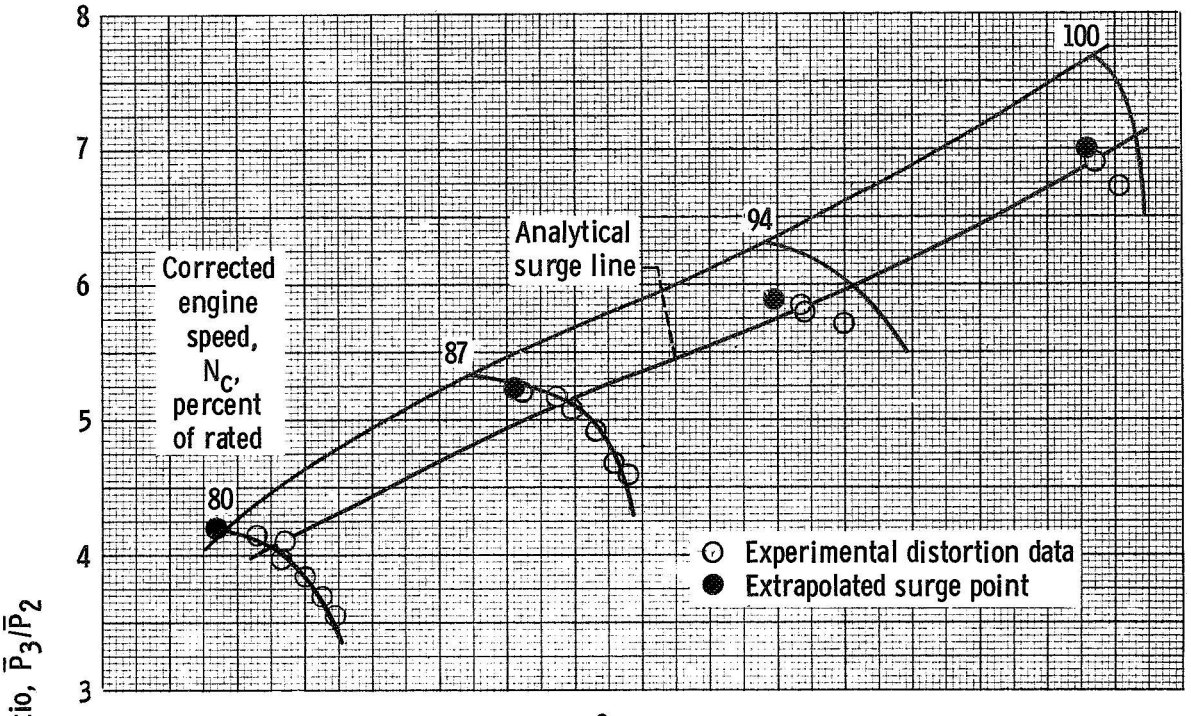

(g) Distortion angle of extent, 60^0; distortion screen density, 49 percent.

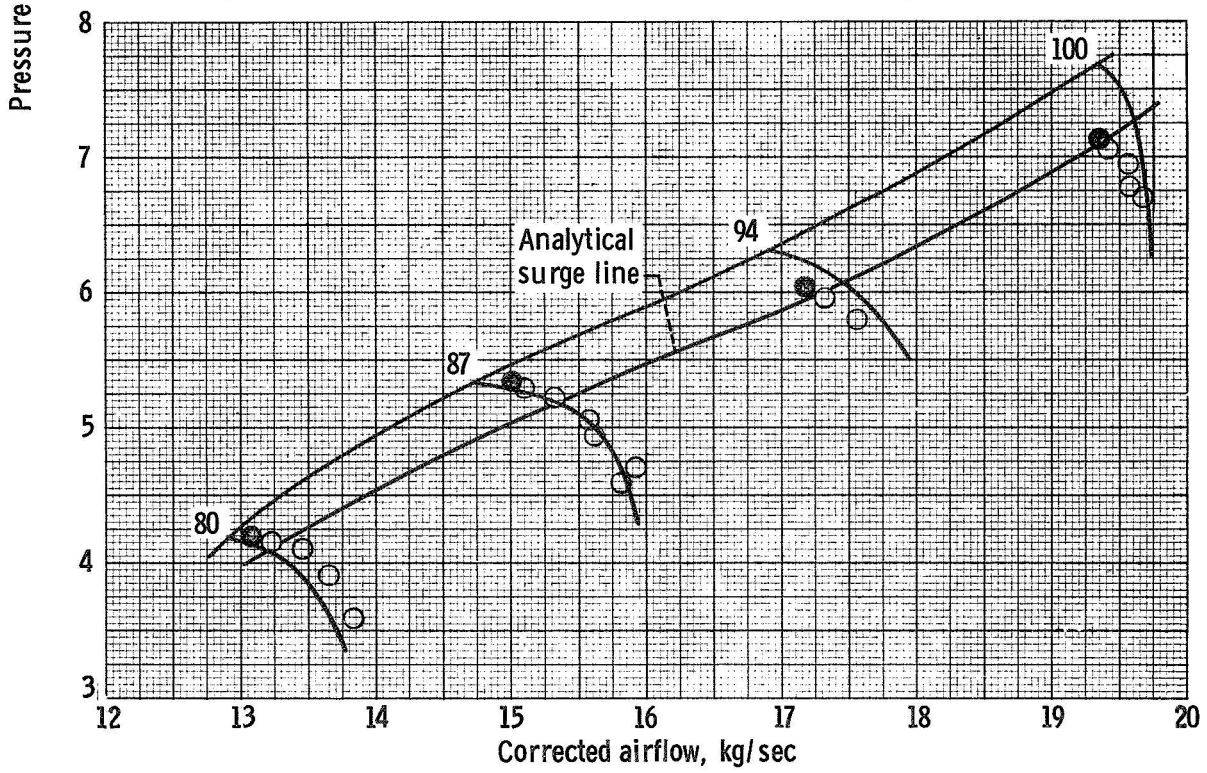

(h) Distortion angle of extent, 60^0; distortion screen density, 42 percent.

Figure 6. - Continued.

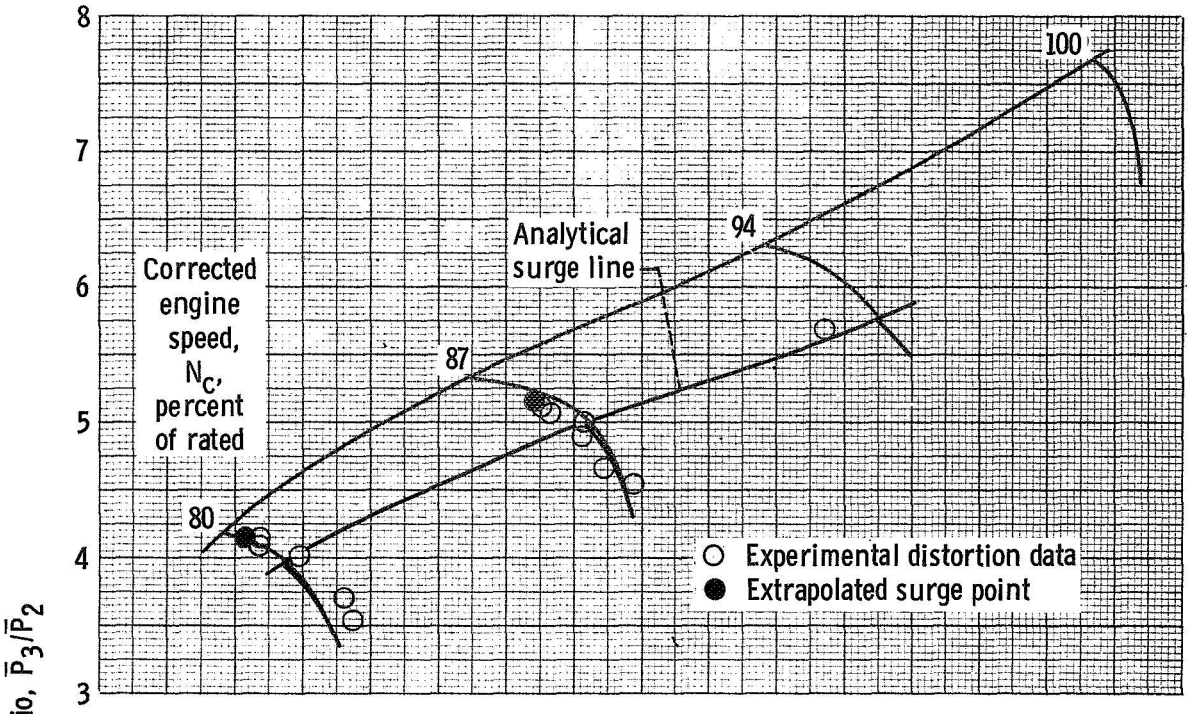

(i) Distortion angle of extent, 60^0; distortion screen density, 69 percent.

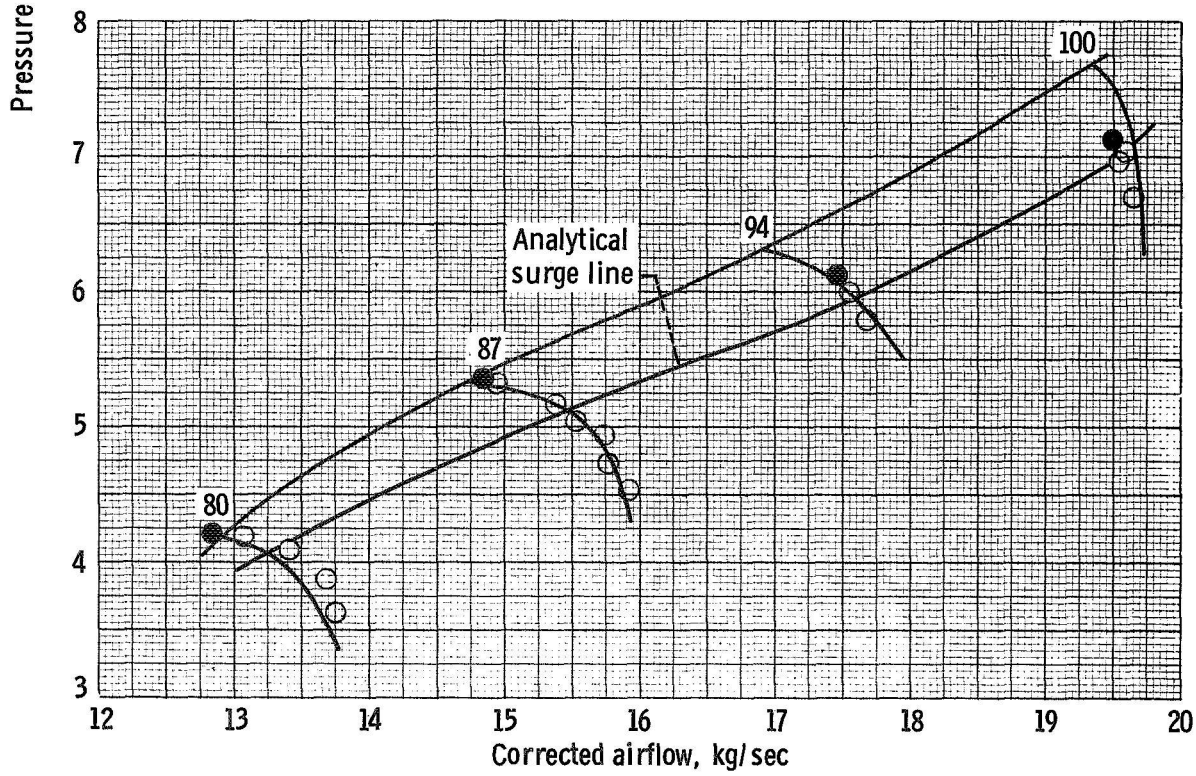

(j) Distortion angle of extent, 30^0; distortion screen density, 42 percent.

Figure 6. - Concluded.

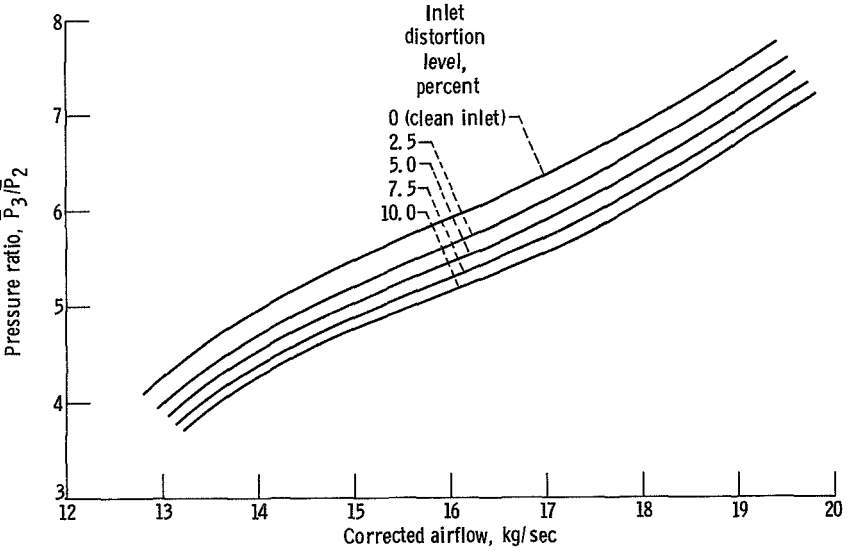

Figure 7. - Predicted compressor surge lines for various inlet-distortion levels using parallel compressor model with 50 percent spoiled area. (Distortion level, $(P_2' - P_{2'}^{1,5})/P_2^*$.)

NATIONAL AERONAUTICS AND SPACE ADMINISTRATION
WASHINGTON, D.C. 20546

OFFICIAL BUSINESS
PENALTY FOR PRIVATE USE $300

SPECIAL FOURTH-CLASS RATE
BOOK

POSTAGE AND FEES PAID
NATIONAL AERONAUTICS AND
SPACE ADMINISTRATION
451

U.S. MAIL

POSTMASTER: If Undeliverable (Section 158
Postal Manual) Do Not Return

"The aeronautical and space activities of the United States shall be conducted so as to contribute . . . to the expansion of human knowledge of phenomena in the atmosphere and space. The Administration shall provide for the widest practicable and appropriate dissemination of information concerning its activities and the results thereof."

—NATIONAL AERONAUTICS AND SPACE ACT OF 1958

NASA SCIENTIFIC AND TECHNICAL PUBLICATIONS

TECHNICAL REPORTS: Scientific and technical information considered important, complete, and a lasting contribution to existing knowledge.

TECHNICAL NOTES: Information less broad in scope but nevertheless of importance as a contribution to existing knowledge.

TECHNICAL MEMORANDUMS: Information receiving limited distribution because of preliminary data, security classification, or other reasons. Also includes conference proceedings with either limited or unlimited distribution.

CONTRACTOR REPORTS: Scientific and technical information generated under a NASA contract or grant and considered an important contribution to existing knowledge.

TECHNICAL TRANSLATIONS: Information published in a foreign language considered to merit NASA distribution in English.

SPECIAL PUBLICATIONS: Information derived from or of value to NASA activities. Publications include final reports of major projects, monographs, data compilations, handbooks, sourcebooks, and special bibliographies.

TECHNOLOGY UTILIZATION PUBLICATIONS: Information on technology used by NASA that may be of particular interest in commercial and other non-aerospace applications. Publications include Tech Briefs, Technology Utilization Reports and Technology Surveys.

Details on the availability of these publications may be obtained from:

SCIENTIFIC AND TECHNICAL INFORMATION OFFICE

NATIONAL AERONAUTICS AND SPACE ADMINISTRATION

Washington, D.C. 20546